

Tucker-O-Minus Decomposition for Multi-view Tensor Subspace Clustering

Yingcong Lu, Yipeng Liu, Zhen Long, Zhangxin Chen, Ce Zhu *

October 25, 2022

Abstract

With powerful ability to exploit latent structure of self-representation information, different tensor decompositions have been employed into low rank multi-view clustering (LRMVC) models for achieving significant performance. However, current approaches suffer from a series of problems related to those tensor decomposition, such as the unbalanced matricization scheme, rotation sensitivity, deficient correlations capture and so forth. All these will lead to LRMVC having insufficient access to global information, which is contrary to the target of multi-view clustering. To alleviate these problems, we propose a new tensor decomposition called Tucker-O-Minus Decomposition (TOMD) for multi-view clustering. Specifically, based on the Tucker format, we additionally employ the O-minus structure, which consists of a circle with an efficient bridge linking two weakly correlated factors. In this way, the core tensor in Tucker format is replaced by the O-minus architecture with a more balanced structure, and the enhanced capacity of capturing the global low rank information will be achieved. The proposed TOMD also provides more compact and powerful representation abilities for the self-representation tensor, simultaneously. The alternating direction method of multipliers is used to solve the proposed model TOMD-MVC. Numerical experiments on six benchmark data sets demonstrate the superiority of our proposed method in terms of F-score, precision, recall, normalized mutual information, adjusted rand index, and accuracy.

1 Introduction

Tensor, a higher order generation of vector and matrix, provides a natural representation for high order data. For example, ORL multi-view data set [54] is a 3rd-order tensor $\mathcal{X}^{I \times C_v \times V}$ ($v = 1, \dots, V$), where I is the number of samples, C_v is the feature size of the v -th view, and V is the number of views. Tensor decomposition allows us to simultaneously explore all dimensions to obtain more

*All the authors are with the School of Information and Communication Engineering, University of Electronic Science and Technology of China (UESTC), Chengdu, 611731, China. E-mail: yipengliu@uestc.edu.cn

latent information, which has attracted attention in a series of fields, e.g., image processing [8, 32], machine learning [15, 16] and signal processing [1, 5]. Tensor-based multi-view clustering (MVC) is one of them, which separates multi-view data into clusters by exploiting their latent information.

Most tensor MVC methods are based on the assumption that their self-representation tensors are low rank [53]. For example, Chen et al. [7] combine the low-rank tensor graph and the subspace clustering into a unified model in multi-view clustering, which applies the Tucker decomposition [41, 42] to explore the low-rank information of representation tensor. With the emergence of a new type of decomposition for 3rd-order tensors [20, 21], multiple multi-view subspace clustering methods based on the tensor singular value decomposition (t-SVD) have been proposed [45, 46, 58]. In addition, tensor networks provide a more compact and flexible representation for higher order tensor than traditional tensor decomposition [27, 30, 31, 33]. In this way, Yu et al. [51] have proposed a novel non-negative tensor ring (NTR) decomposition and graph-regularized NTR (GNTR) for the non-negative multi-way representation learning with satisfying performance in clustering tasks.

Although the aforementioned methods have achieved promising clustering performance, there are still several problems. Since the Tucker rank is related to the unbalanced mode- n unfolding matrices [2], capturing the global information of the self-representation tensor by simply processing Tucker decomposition may be difficult in LRMVC. Besides, the t-SVD suffers from rotation sensitivity and the low rank information can not be fully discovered in the 3rd mode [10]. Thus, the t-SVD based methods always need to utilize the rotation operation of the self-representation tensor to explore the correlations across different views. Naturally, the acquisition of the correlations among samples will be inadequate. Furthermore, tensor ring (TR) has shown better performance in exploring the low-rank information with the well-balanced matricization scheme. However, the interaction of neighboring modes in TR is stronger than that of two modes separated by a large distance, whose correlations are also have been ignored.

Considering the above problems, we propose the Tucker-O-Minus decomposition for multi-view subspace clustering. For employing the additional factors and correlations to construct a more compact and balanced tensor network, a simple way seems to replace the core factor of the Tucker structure with the TR format. However, as we mentioned above, the TR architecture suffers from a deficiency in exploring the correlations between the weakly-connected modes, which will result in the loss of essential clustering information in LRMVC. To this end, we propose the O-minus structure for LRMVC in the following three considerations. Firstly, from the perspective of two-point correlations in high-energy physics [3], appending moderate lines with effective vertexes between two slightly correlated factors will strengthen their relationships. Similarly, we try to add the "bridge" with a tensor factor based on the TR structure to better capture the low rank information. Nonetheless, more links will generate more loops, which will cause huge difficulties in tensor contraction and the computational complexity burden of the tensor networks [9]. Simultaneously, since the number of samples $I \gg V$ in LRMVC, compared with higher-order information

across different views, the information related to the correlations of instances requires more connections to be fully discovered. Accordingly, to efficiently explore the low rank information in LRMVC, the correlations related to samples (i.e., I_1 , and I_3 in Fig. 1) are further strengthened by the special "bridge". This unique internal architecture is similar to " \ominus ", thus namely O-Minus. And the whole architecture called Tucker-O-Minus decomposition is illustrated in Fig. 1. In this way, the low rank based multi-view clustering problem can be successfully solved with satisfying results. The main contributions of this paper are summarized as follows:

1. We propose the Tucker-O-Minus decomposition. Different from the existing tensor networks, it allows more valid interaction among nonadjacent factors and obtains a better low rank representation for high-dimensional data. Numerical experimental results on gray image reconstruction show that the performance of TOMD in exploring low rank information is superior to others.
2. We apply TOMD to a unified multi-view clustering framework. The proposed model, namely TOMD-MVC, utilizes the TOMD to capture the low-rank properties of self-representation tensor from multi-view data. The alternating direction method of multipliers (ADMM) is applied to solve the optimization model.
3. We conduct extensive experiments on six real-world multi-view data sets to demonstrate the performance of our method. Compare with state-of-the-art models, TOMD-MVC achieves highly competitive or even better performance in terms of six evaluation metrics.

The remainder of this paper is organized as follows. Section 2 gives the used notations, mathematical backgrounds, and review the related works. The proposed tensor network is presented in details in Section 3. Section 4 gives the multi-view clustering method based on the newly proposed tensor network. The experimental results are demonstrated and analyzed in Section 5. Section 6 draws the conclusion finally.

2 Notations, Preliminaries, and Related Works

2.1 Notations

We give a brief introduction about notations and preliminaries in this section. Throughout this paper, we use lower case letters, bold lower case letters, bold upper case letters, and calligraphic letters to denote scalars, vectors, matrices and tensors, respectively, e.g., a , \mathbf{a} , \mathbf{A} and \mathcal{A} . Some other frequently used notations are listed in Table 1, where \mathcal{A} is a 3rd-order tensor and \mathbf{A} is a matrix.

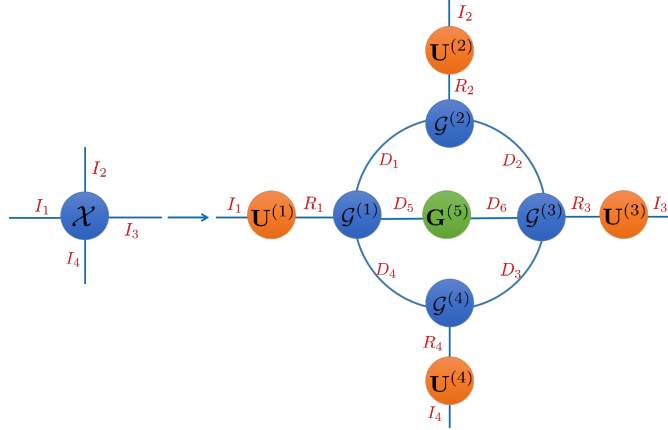


Figure 1: The graphical illustration of TOMD for a 4th-order tensor $\mathcal{X} \in \mathbb{R}^{I_1 \times I_2 \times I_3 \times I_4}$, where $\mathbf{U}^{(i)} \in \mathbb{R}^{I_i \times R_i}$ ($i = 1, \dots, 4$) are factor matrices, $\mathcal{G}^{(n)}$, $n = 1, \dots, 5$, are the sub-tensors.

Table 1: Summary of notations in this paper.

Denotation	Definition
\mathbf{A}_i	$\mathbf{A}_i = \mathcal{A}(:, :, i)$
a_{i_1, i_2, i_3}	The (i_1, i_2, i_3) -th entry of tensor \mathcal{A}
$\text{tr}(\mathbf{A})$	$\text{tr}(\mathbf{A}) = \sum_i a_{i, i}$
$\ \mathbf{A}\ _{\text{F}}$	$\ \mathbf{A}\ _{\text{F}} = \sqrt{\sum_{i_1 i_2} a_{i_1, i_2}^2}$
$\ \mathbf{A}\ _{\infty}$	$\ \mathbf{A}\ _{\infty} = \max_{i_1 i_2} \mathbf{A}_{i_1, i_2} $
$\ \mathbf{A}\ _{2,1}$	$\ \mathbf{A}\ _{2,1} = \sum_j \ \mathbf{A}(:, j)\ _2$
$\ \mathcal{A}\ _{\text{F}}$	$\ \mathcal{A}\ _{\text{F}} = \sqrt{\sum_{i_1 i_2 i_3} a_{i_1, i_2, i_3} ^2}$

2.2 Preliminaries

Definition 1. (Mode- n unfolding) [22] For tensor $\mathcal{A} \in \mathbb{R}^{I_1 \times \dots \times I_N}$, its matricization along the n -th mode is denoted as $\mathbf{A}_{(n)} \in \mathbb{R}^{I_n \times I_1 I_2 \dots I_{n-1} I_{n+1} \dots I_N}$.

Definition 2. (n -unfolding) [9] Given an N -way tensor $\mathcal{A} \in \mathbb{R}^{I_1 \times \dots \times I_N}$, the definition of its n -unfolding is expressed as $\mathbf{A}_{(n)} \in \mathbb{R}^{I_1 \dots I_n \times I_{n+1} \dots I_N}$.

Definition 3. (Mode- n product) [22] The mode- n product of $\mathcal{A} \in \mathbb{R}^{I_1 \times \dots \times I_N}$ and matrix $\mathbf{B} \in \mathbb{R}^{J \times I_n}$ is defined as

$$\mathcal{X} = \mathcal{A} \times_n \mathbf{B} \in \mathbb{R}^{I_1 \times \dots \times I_{n-1} \times J \times I_{n+1} \times \dots \times I_N}. \quad (1)$$

Definition 4. (Tensor Network Contraction) [38] Given a tensor network composed of N sub-tensors $\{\mathcal{G}^{(n)}\} (n = 1, \dots, N)$, then \mathcal{G} is denoted as the tensor network contraction result of $\{\mathcal{G}^{(n)}\} (n = 1, \dots, N)$, whose general mathematical equation can be written as

$$\begin{aligned} \mathcal{G} &= \sum_{n=1}^N \sum_{r_1^n, r_2^n, \dots}^{R_1^n, R_2^n, \dots} \left\{ \sum_{d_1, d_2, \dots}^{D_1, D_2, \dots} \prod_{n=1}^N \mathcal{G}^{(n)}(\{r_1^n, r_2^n, \dots, d_1, d_2, \dots\}) \right\} \\ &= \text{TC}(\{\mathcal{G}^{(n)}\}_{n=1}^N), \end{aligned} \quad (2)$$

where $\{D_1, D_2, \dots\}$ are geometrical indexes, each of which is shared normally two tensors and will be contracted, $\mathbb{R} = \{R_1^1, R_2^1, \dots, R_1^N, R_2^N, \dots\}$ are open bounds, each of which only belongs to one tensor. After contracting all the geometrical indexes, the \mathcal{G} represents a P -th order tensor with P the total number of the open indexes \mathbb{R} .

2.3 Related Works

This section reviews some closely related works, including low-rank approximation based multi-view subspace clustering, and multi-view graph clustering.

2.3.1 Low-rank Approximation Based Multi-view Subspace Clustering

Subspace learning based multi-view clustering methods assume that each sample can be represented as a linear combination of all the samples [40].

Chen et al. [7] utilize the Tucker decomposition to obtain the "clean" representation tensor from view specific matrices. He et al. [12] introduce a tensor-based multi-linear multi-view clustering (MMC) method. Under the consideration of Canonical Polyadic Decomposition (CPD) [19], the MMC is able to explore the higher-order interaction information among the multiple views. Recently, tensor singular value decomposition (t-SVD) based tensor nuclear norm [20, 21] shows satisfying performance in capturing low rank information for 3rd-order tensor. Thus, many t-SVD based works [45, 46, 48] are proposed for better capturing the high-order correlation hidden in 3rd-order tensor from

multi-view data. To preserve the consensus across different views, Xie et al. [48] proposed the t-SVD-MSC model, which adopts the t-SVD based tensor nuclear norm to LRMVC. Consider that those self-representation based subspace clustering method will lead to high computation complexity, the essential tensor learning for multi-view spectral clustering (ETLMSC) [45] with Markov chain based spectral clustering and the unified graph and low-rank tensor learning (UGLTL) [46] have been proposed. Zheng et al. [59] develop a bi-linear factorization based clustering method with the orthogonality and low-rank constraint to effectively explore the consensus information of multi-view data. Work in [47] develops the tensorized bipartite graph learning for multi-view clustering (TBGL), which considers the inter-view and intra-view similarities with tensor Schatten p -norm and $\ell_{1,2}$ -norm penalty, respectively. Yu et al. [51] propose NTR decomposition and the GNTR decomposition, which yield better performance than the state-of-the-art tensor based methods in clustering.

2.3.2 Multi-view Graph Clustering

Graph learning based multi-view clustering obtains a fusion graph across all views and uses the standard clustering algorithm to produce the final clusters [50]. Given a multi-view dataset, which has V multiple views $\{\mathbf{X}_v \in \mathbb{R}^{C_v \times N}\}$ ($v = 1, \dots, V$), a general multi-view graph clustering optimization model can be formulated as follows:

$$\begin{aligned} \min_{\mathbf{M}_i} \sum_{v=1}^V \sum_{j=1}^N \frac{1}{2} \|(\mathbf{X}_i)_v - (\mathbf{X}_j)_v\|_2^2 m_{i,j} + \lambda \sum_{j=1}^N m_{i,j}^2 \\ \text{s. t. } \mathbf{M}_i^T \mathbf{1} = \mathbf{1}, 0 \leq m_{i,j} \leq 1, \end{aligned} \quad (3)$$

where $\mathbf{M} \in \mathbb{R}^{N \times N}$ is the affinity matrix, \mathbf{M}_i is the i -th column of matrix \mathbf{M} , $(\mathbf{X}_i)_v$ denotes the i -th column of \mathbf{X}_v , and λ is the trade-off parameter.

By defining the graph Laplacian matrix $\mathbf{L} = \mathbf{D} - (\mathbf{M} + \mathbf{M}^T)/2$, where \mathbf{D} is a diagonal matrix whose i -th diagonal entry is $\sum_j (m_{i,j} + m_{j,i})/2$, (3) can be rewritten as

$$\begin{aligned} \min_{\mathbf{M}} \sum_{v=1}^V \text{tr}(\mathbf{X}_v \mathbf{L} \mathbf{X}_v^T) + \lambda \|\mathbf{M}\|_F^2 \\ \text{s. t. } \mathbf{M}^T \mathbf{1} = \mathbf{1}, \mathbf{0} \leq \mathbf{M} \leq \mathbf{1}. \end{aligned} \quad (4)$$

Based on (4), works in [13,36,37,61] use a parameter-free multiple graph clustering model to automatically learn the optimal weight for graphs. Moreover, Nie et al. introduce a multi-view learning model with adaptive neighbors [35], which simultaneously performs clustering and local structure learning. Wang et al. introduce a general graph-based multi-view clustering (GMC) method [43], which does not only obtain the final clusters directly but also constructs the graph of each view and the fusion graph jointly, thus they can help each other mutually.

3 Tucker-O-Minus Decomposition

In this section, the mathematical formulation of Tucker-O-Minus decomposition with its corresponding solution is given in details.

3.1 Decomposition Formulation

Given a 4th-order tensor $\mathcal{X} \in \mathbb{R}^{I_1 \times I_2 \times I_3 \times I_4}$, the mathematical formulation of the TOMD is as follows:

$$\begin{aligned} \mathcal{X} = & \left\{ \sum_{r_1, \dots, r_4}^{R_1, \dots, R_4} \left(\sum_{d_1, \dots, d_6}^{D_1, \dots, D_6} \mathcal{G}^{(1)}(d_4, r_1, d_1, d_5) \mathcal{G}^{(2)}(d_1, r_2, d_2) \right. \right. \\ & \left. \left. \mathcal{G}^{(3)}(d_2, r_3, d_3, d_6) \mathcal{G}^{(4)}(d_3, r_4, d_4) \mathbf{G}^{(5)}(d_5, d_6) \right) \right\} \\ & \times_1 \mathbf{U}^{(1)} \times_2 \mathbf{U}^{(2)} \times_3 \mathbf{U}^{(3)} \times_4 \mathbf{U}^{(4)} \\ = & \text{TC}(\{\mathcal{G}^{(n)}\}_{n=1}^5) \times_1 \mathbf{U}^{(1)} \times_2 \mathbf{U}^{(2)} \times_3 \mathbf{U}^{(3)} \times_4 \mathbf{U}^{(4)}, \end{aligned} \quad (5)$$

where $\{D_1, \dots, D_6\}$ are geometrical indexes, each of which is shared two tensors and should be contracted. $\mathbf{U}^{(i)} \in \mathbb{R}^{I_i \times R_i}$ ($i = 1, \dots, 4$) are factor matrices, $\mathcal{G}^{(n)}$, $n = 1, \dots, 5$, are the factor tensors. Specifically, $\mathcal{G}^{(1)} \in \mathbb{R}^{D_4 \times R_1 \times D_1 \times D_5}$, $\mathcal{G}^{(2)} \in \mathbb{R}^{D_1 \times R_2 \times D_2}$, $\mathcal{G}^{(3)} \in \mathbb{R}^{D_2 \times R_3 \times D_3 \times D_6}$, $\mathcal{G}^{(4)} \in \mathbb{R}^{D_3 \times R_4 \times D_4}$, and $\mathbf{G}^{(5)} \in \mathbb{R}^{D_5 \times D_6}$. $[R_1, \dots, R_4, D_1, \dots, D_6]^T$ is denoted as the rank of TOMD.

From the graphical illustration of TOMD in Fig. 1, it can be clearly seen that the overall architecture of our proposed tensor network is relatively compact and balanced. In this way, based on the Tucker format, O-minus structure is further applied to enhance the relationships among the adjacent and non-adjacent modes of \mathcal{X} , simultaneously. In addition, the computational complexity of tensor network contraction can be controlled.

3.2 ALS algorithm

To compute the Tucker-O-Minus decomposition, we employ the alternation least squares (ALS) algorithm, which has been widely used for CPD, Tucker decomposition and TR decomposition [4, 23, 57]. Supposing that we have a 4th-order tensor $\mathcal{X} \in \mathbb{R}^{I_1 \times I_2 \times I_3 \times I_4}$, the optimization model for approximation a tensor \mathcal{X} by the proposed TOMD can be formulated as follows:

$$\min_{\substack{\{\mathcal{G}^{(n)}\}_{n=1}^5 \\ \{\mathbf{U}^{(n)}\}_{n=1}^4}} \|\mathcal{X} - \text{TC}(\{\mathcal{G}^{(n)}\}_{n=1}^5) \times_1 \mathbf{U}^{(1)} \times_2 \dots \times_4 \mathbf{U}^{(4)}\|_{\text{F}}. \quad (6)$$

Theorem 1. *Given a Tucker-O-Minus decomposition $\mathcal{X} = \text{TC}(\{\mathcal{G}^{(n)}\}_{n=1}^5) \times_1 \mathbf{U}^{(1)} \times_2 \mathbf{U}^{(2)} \times_3 \mathbf{U}^{(3)} \times_4 \mathbf{U}^{(4)}$, the corresponding mode- n unfolding based matrix equivalence of (5) can be written as $\mathbf{X}_{(n)} = \mathbf{U}^{(n)}(\mathbf{A}_{(n)})$, or $\mathbf{X}_{(n)} = \mathbf{U}^{(n)}(\mathbf{G}_{(2)}^{(n)})(\mathbf{A}^{\neq n})$, where $\mathbf{A}^{\neq n} = \mathbf{A}_{(3)}^{\neq n}$ ($n = 1$ or 3), and $\mathbf{A}^{\neq n} = \mathbf{A}_{(2)}^{\neq n}$ ($n = 2$ or 4). Moreover, we have $\mathcal{A} = \mathcal{G} \times_1 \mathbf{U}^{(1)} \dots \times_{n-1} \mathbf{U}^{(n-1)} \times_{n+1} \mathbf{U}^{(n+1)} \dots \times_4 \mathbf{U}^{(4)}$, and*

$\mathcal{A} = \mathcal{G} \times_1 \mathbf{U}^{(1)} \cdots \times_{n-1} \mathbf{U}^{(n-1)} \times_{n+1} \mathbf{U}^{(n+1)} \cdots \times_4 \mathbf{U}^{(4)}$, respectively, where $\mathcal{G} = \text{TC}(\{\mathcal{G}^{(n)}\}_{n=1}^5)$ and $\mathcal{G}^{\neq n} = \text{TC}(\{\mathcal{G}^{(n_1)}\}_{n_1 \neq n}^5)$. $\mathbf{A}_{(2)}^{\neq n}$ and $\mathbf{A}_{(3)}^{\neq n}$ are the n -unfolding matrices of $\mathcal{A}^{\neq n}$.

Theorem 2. Suppose that we have a Tucker-O-Minus decomposition $\mathcal{X} = \text{TC}(\{\mathcal{G}^{(n)}\}_{n=1}^5) \times_1 \mathbf{U}^{(1)} \times_2 \mathbf{U}^{(2)} \times_3 \mathbf{U}^{(3)} \times_4 \mathbf{U}^{(4)}$, and its vectorized form can be formulated as $\mathbf{x} = \mathbf{g}^{(5)} \tilde{\mathbf{A}}_{(2)}$, where $\mathbf{x} \in \mathbb{R}^{1 \times I_1 I_2 I_3 I_4}$, $\mathbf{g}^{(5)} \in \mathbb{R}^{1 \times D_5 D_6}$ are the vectorized form of \mathcal{X} and $\mathbf{G}^{(5)}$, respectively. Furthermore, $\tilde{\mathbf{A}}$ can be calculated by $\tilde{\mathbf{A}} = \mathcal{G}^{\neq 5} \times_3 \mathbf{U}^{(1)} \times_4 \cdots \times_6 \mathbf{U}^{(4)} \in \mathbb{R}^{D_5 \times D_6 \times I_1 \times \cdots \times I_4}$, where $\mathcal{G}^{\neq 5} = \text{TC}(\{\mathcal{G}^{(n)}\}_{n=1}^4) \in \mathbb{R}^{D_5 \times D_6 \times R_1 \times R_2 \times R_3 \times R_4}$. $\tilde{\mathbf{A}}_{(2)}$ is the n -unfolding of $\tilde{\mathbf{A}}$.

From Fig. 1, Theorem 1 and Theorem 2, the optimization problem (6) can be changed into a few subproblems by alternating least squares method. In detail, fixing all but one factor, the problem can reduce to three least-squares problems:

1. Subproblem with respect to $\mathbf{U}^{(n)} (n = 1, \dots, 4)$:

$$\min_{\mathbf{U}^{(n)}} \|\mathbf{X}_{(n)} - \mathbf{U}^{(n)}(\mathbf{A}_{(n)})\|_{\text{F}}. \quad (7)$$

2. Subproblem with respect to $\mathcal{G}^{(n)} (n = 1, \dots, 4)$:

$$\min_{\mathbf{G}^{(n)}} \|\mathbf{X}_{(n)} - \mathbf{U}^{(n)}(\mathbf{G}_{(2)}^{(n)})(\mathbf{A}^{\neq n})\|_{\text{F}}. \quad (8)$$

3. Subproblem with respect to $\mathcal{G}^{(5)}$:

$$\min_{\mathbf{g}^{(5)}} \|\mathbf{x} - (\mathbf{g}^{(5)}) \tilde{\mathbf{A}}_{(2)}\|_{\text{F}}. \quad (9)$$

Moreover, 9 factors (i.e., $\{\mathcal{G}^{(n)}\}_{n=1}^5, \{\mathbf{U}^{(n)}\}_{n=1}^4$) can be initialized using the randomization method or truncated SVD with specific values of ranks. In our experiments, we choose the latter way to initialize all factors, and the stopping condition is $\|\mathcal{X}_{\text{last}} - \mathcal{X}_{\text{new}}\|_{\text{F}} / \|\mathcal{X}_{\text{last}}\|_{\text{F}} \leq \text{tol}_{\text{als}}$, where $\mathcal{X}_{\text{last}}$ is the value at the last iteration, \mathcal{X}_{new} is constructed from the new iteration, and tol_{als} is a predefined threshold.

By denoting $\Phi(\cdot, \mathbf{s})$ as an operator that reshapes a tensor using the size vector \mathbf{s} , the overall procedure of TOMD-ALS algorithm can be found in Algorithm 1.

4 Tucker-O-Minus decomposition for low rank multi-view clustering model

In this section, we firstly apply TOMD into the low rank tensor optimization model for multi-view clustering. The alternating direction method of multipliers is used to solve it. And its computational complexity is briefly analyzed.

Algorithm 1 TOMD-ALS

Input: A 4th-order data tensor $\mathcal{X} \in \mathbb{R}^{I_1 \times I_2 \times I_3 \times I_4}$, predefined TOMD rank, maximum number of iterations (iter_{\max}), and the threshold for stopping the algorithm $\text{tol}_{\text{als}} = 10^{-12}$, $f_1 = 0$, $i = 0$.

Initialization: Initialize $\mathcal{G}^{(1)}, \dots, \mathcal{G}^{(4)}, \mathbf{G}^{(5)}, \mathbf{U}^{(1)}, \dots, \mathbf{U}^{(4)}$.

$\mathcal{X}_{\text{new}} = \mathcal{G} \times_1 \mathbf{U}^{(1)} \times_2 \dots \times_4 \mathbf{U}^{(4)}$;

while $i \leq \text{iter}_{\max}$ **do**

$\mathcal{X}_{\text{last}} = \mathcal{X}_{\text{new}}$;

for $n = 1 : 4$ **do**

$\mathbf{A} = \mathcal{G} \times_1 \mathbf{U}^{(1)} \dots \times_{n-1} \mathbf{U}^{(n-1)} \times_{n+1} \mathbf{U}^{(n+1)} \dots \times_4 \mathbf{U}^{(4)}$;

$\mathbf{U}^{(n)} \leftarrow \arg \min \|\mathbf{X}_{(n)} - \mathbf{U}^{(n)}(\mathbf{A}_{(n)})\|_{\text{F}}$;

end for

for $n = 1 : 4$ **do**

$\mathbf{A}^{\neq n} = \mathcal{G}^{\neq n} \times_1 \mathbf{U}^{(1)} \times_2 \dots \times_{n-1} \mathbf{U}^{(n-1)} \times_{n+1} \mathbf{U}^{(n+1)} \times_{n+2} \dots \times_4 \mathbf{U}^{(4)}$;

$\mathbf{G}_{(2)}^{(n)} \leftarrow \arg \min \|\mathbf{X}_{(n)} - \mathbf{U}^{(n)}(\mathbf{G}_{(2)}^{(n)})(\mathbf{A}^{\neq n})\|_{\text{F}}$;

$\mathcal{G}^{(n)} = \Phi(\mathbf{G}_{(2)}^{(n)}, \text{size}(\mathcal{G}^{(n)}))$;

end for

$\tilde{\mathcal{A}} = \mathcal{G}^{\neq 5} \times_1 \mathbf{U}^{(1)} \times_2 \dots \times_4 \mathbf{U}^{(4)}$;

$\tilde{\mathbf{A}} = \Phi(\tilde{\mathcal{A}}, [\sim, I_1 \dots I_4])$, $\mathbf{x} = \Phi(\mathcal{X}, [\sim, I_1 \dots I_4])$;

$\mathbf{g}^{(5)} \leftarrow \arg \min \|\mathbf{x} - (\mathbf{g}^{(5)})\tilde{\mathbf{A}}_{(2)}\|_{\text{F}}$;

$\mathbf{G}^{(5)} = \Phi(\mathbf{g}^{(5)}, \text{size}(\mathcal{G}^{(5)}))$;

$\mathcal{X}_{\text{new}} = \mathcal{G} \times_1 \mathbf{U}^{(1)} \times_2 \dots \times_4 \mathbf{U}^{(4)}$;

$f_1 = \frac{\|\mathcal{X}_{\text{last}} - \mathcal{X}_{\text{new}}\|_{\text{F}}}{\|\mathcal{X}_{\text{last}}\|_{\text{F}}}$;

if $f_1 \leq \text{tol}_{\text{als}}$ **then**

 break

end if

$i = i + 1$;

end while

Output: $\mathcal{G}^{(1)}, \dots, \mathcal{G}^{(4)}, \mathbf{G}^{(5)}, \mathbf{U}^{(1)}, \dots, \mathbf{U}^{(4)}$.

4.1 Optimization Model

To better exploit the low rank data structure in multi-view clustering, we apply the proposed TOMD to the optimization model for clustering. Given a dataset that has V views $\{\mathbf{X}_v \in \mathbb{R}^{C_v \times N}\}$, $v = 1, \dots, V$, where C_v is the feature dimension of the v -th feature and N is the number of data samples in each view. The proposed optimization model based on TOMD for multi-view cluster

(TOMD-MVC) can be formulated as follows:

$$\begin{aligned}
& \min_{\{\mathcal{G}^{(n)}\}_{n=1}^5, \{\mathbf{U}^{(n)}\}_{n=1}^4, \mathbf{Z}, \mathbf{E}, \mathbf{M}} \mu \sum_{v=1}^V \text{tr}(\mathbf{Z}_v^T \mathbf{L} \mathbf{Z}_v) + \lambda \|\mathbf{M}\|_{\text{F}}^2 + \|\mathbf{E}\|_{2,1} \\
& \text{s. t. } \mathbf{X}_v = \mathbf{X}_v \mathbf{Z}_v + \mathbf{E}_v, \quad v = 1, 2, \dots, V, \\
& \mathbf{M}^T \mathbf{1} = \mathbf{1}, \mathbf{0} \leq \mathbf{M} \leq \mathbf{1}, \\
& \mathcal{Z} = \Phi(\text{TC}(\{\mathcal{G}^{(n)}\}_{n=1}^5) \times_1 \mathbf{U}^{(1)} \dots \times_4 \mathbf{U}^{(4)}, [N, N, V]), \\
& \mathcal{Z} = \Omega(\mathbf{Z}_1, \mathbf{Z}_2, \dots, \mathbf{Z}_V), \mathbf{E} = [\mathbf{E}_1; \mathbf{E}_2; \dots; \mathbf{E}_V],
\end{aligned} \tag{10}$$

where $\{\mathcal{G}^{(n)}\}_{n=1}^5$ are tensor factors, and \mathbf{L} is the graph Laplacian matrix of \mathbf{M} . $\mathbf{E} = [\mathbf{E}_1; \mathbf{E}_2; \dots; \mathbf{E}_V]$ makes all the error matrices $\{\mathbf{E}_v\}$ ($v = 1, \dots, V$) vertically connected along the columns, and function $\Omega(\cdot)$ constructs the matrices $\{\mathbf{Z}_v\}$ ($v = 1, \dots, V$) into a 3rd-order tensor. Apart from that, μ and λ are positive penalty scalars.

After obtaining the affinity matrix \mathbf{M} , K-means [11], spectral clustering [34] and other clustering methods can be utilized to yield the final clustering results.

4.2 Solution

The optimization problem (10) can be solved by ADMM. Since variable \mathcal{Z} has appeared in the objective function and three constraints simultaneously, we introduce an extra variable \mathcal{S} to make \mathcal{Z} separable, which result in the equivalence of (10) as follows:

$$\begin{aligned}
& \min_{\{\mathcal{G}^{(n)}\}_{n=1}^5, \{\mathbf{U}^{(n)}\}_{n=1}^4, \mathcal{Z}, \mathbf{E}, \mathbf{M}} \mu \sum_{v=1}^V \text{tr}(\mathbf{Z}_v^T \mathbf{L} \mathbf{Z}_v) + \lambda \|\mathbf{M}\|_{\text{F}}^2 + \|\mathbf{E}\|_{2,1} \\
& \text{s. t. } \mathbf{X}_v = \mathbf{X}_v \mathbf{S}_v + \mathbf{E}_v, \quad v = 1, 2, \dots, V, \\
& \mathbf{M}^T \mathbf{1} = \mathbf{1}, \mathbf{0} \leq \mathbf{M} \leq \mathbf{1}, \\
& \mathcal{Z} = \Phi(\text{TC}(\{\mathcal{G}^{(n)}\}_{n=1}^5) \times_1 \mathbf{U}^{(1)} \dots \times_4 \mathbf{U}^{(4)}, [N, N, V]), \\
& \mathcal{Z} = \mathcal{S}, \\
& \mathcal{Z} = \Omega(\mathbf{Z}_1, \mathbf{Z}_2, \dots, \mathbf{Z}_V), \mathbf{E} = [\mathbf{E}_1; \mathbf{E}_2; \dots; \mathbf{E}_V].
\end{aligned} \tag{11}$$

The augmented Lagrangian function of optimization model (11) is

$$\begin{aligned}
L(\mathcal{Z}, \mathcal{S}, \mathbf{E}, \mathbf{M}; \mathcal{W}, \mathcal{Y}) &= \lambda \|\mathbf{M}\|_{\text{F}}^2 + \|\mathbf{E}\|_{2,1} + \sum_{v=1}^V (\mu \text{tr}(\mathbf{S}_v^T \mathbf{L} \mathbf{S}_v) \\
&+ \langle \mathbf{W}_v, \mathbf{X}_v - \mathbf{X}_v \mathbf{S}_v - \mathbf{E}_v \rangle + \frac{\tau}{2} \|\mathbf{X}_v - \mathbf{X}_v \mathbf{S}_v - \mathbf{E}_v\|_{\text{F}}^2) \\
&+ \langle \mathcal{Y}, \mathcal{Z} - \mathcal{S} \rangle + \frac{\tau}{2} \|\mathcal{Z} - \mathcal{S}\|_{\text{F}}^2,
\end{aligned} \tag{12}$$

where \mathcal{W} and \mathcal{Y} are Lagrangian multipliers corresponding to two equations, $\langle \cdot, \cdot \rangle$ denotes the inner product, and τ is the penalty parameter. ADMM alternately updates each variable as follows.

Solving \mathcal{Z} -subproblem: With the other variables fixed but let \mathcal{Z} be the optimization variable, (11) becomes

$$\begin{aligned} \min_{\mathcal{Z}, \{\mathcal{G}^{(n)}\}_{n=1}^5, \{\mathbf{U}^{(n)}\}_{n=1}^4} & \|\mathcal{Z} - (\mathcal{S}^t - \frac{\mathcal{Y}^t}{\tau^t})\|_{\mathbb{F}}^2 \\ \text{s. t. } \mathcal{Z} = & \Phi(\text{TC}(\{\mathcal{G}^{(n)}\}_{n=1}^5) \times_1 \mathbf{U}^{(1)} \cdots \times_4 \mathbf{U}^{(4)}, [N, N, V]), \end{aligned} \quad (13)$$

where t is the number of iteration. This problem can be solved by TOMD-ALS to obtain the factors $\tilde{\mathcal{G}}^{(i)} (i = 1, \dots, 5)$ and $\tilde{\mathbf{U}}^{(i)} (i = 1, \dots, 4)$ of tensor $(\mathcal{S}^t - \frac{\mathcal{Y}^t}{\tau^t})$. Accordingly, the \mathcal{Z} -subproblem has following solution:

$$\mathcal{Z}^{t+1} = \Phi(\text{TC}(\{\tilde{\mathcal{G}}^{(n)}\}_{n=1}^5) \times_1 \tilde{\mathbf{U}}^{(1)} \times_2 \cdots \times_4 \tilde{\mathbf{U}}^{(4)}, [N, N, V]). \quad (14)$$

Solving \mathcal{S} -subproblem: Similarly, letting \mathcal{S} be the only variable, (11) becomes

$$\begin{aligned} \mathcal{S}^{t+1} = \operatorname{argmin}_{\mathcal{S}} & \sum_{v=1}^V \left(\frac{\tau^t}{2} \|\mathbf{X}_v - \mathbf{X}_v \mathbf{S}_v - \mathbf{E}_v + \frac{\mathbf{W}_v^t}{\tau^t}\|_{\mathbb{F}}^2 \right. \\ & \left. + \mu \operatorname{tr}(\mathbf{S}_v^T \mathbf{L} \mathbf{S}_v) \right) + \frac{\tau^t}{2} \|\mathcal{Z}^{t+1} - \mathcal{S} + \frac{\mathcal{Y}^t}{\tau^t}\|_{\mathbb{F}}^2. \end{aligned} \quad (15)$$

By separating above problem into V subproblems, each of which can be solved by:

$$\begin{aligned} \mathbf{S}_v^{t+1} = & (\tau^t (\mathbf{t} + \mathbf{X}_v^T \mathbf{X}_v) + 2\mu \mathbf{L})^{-1} (\tau^t \mathbf{Z}_v^{t+1} \\ & + \mathbf{Y}_v^t + \tau^t \mathbf{X}_v^T (\mathbf{X}_v - \mathbf{E}_v + \frac{\mathbf{W}_v^t}{\tau^t})). \end{aligned} \quad (16)$$

Solving \mathbf{E} -subproblem: The optimization subproblem with respect to \mathbf{E} is:

$$\begin{aligned} \mathbf{E}^{t+1} = \operatorname{argmin}_{\mathbf{E}} & \frac{1}{\tau^t} \|\mathbf{E}\|_{2,1} \\ & + \frac{1}{2} \sum_{v=1}^V \|\mathbf{E}_v - (\mathbf{X}_v - \mathbf{X}_v \mathbf{S}_v^{t+1} + \frac{\mathbf{W}_v^t}{\tau^t})\|_{\mathbb{F}}^2. \end{aligned} \quad (17)$$

Let $\mathbf{H}_v^t = \mathbf{X}_v - \mathbf{X}_v \mathbf{S}_v^{t+1} + \frac{\mathbf{W}_v^t}{\tau^t}$, then \mathbf{H}^t is constructed by vertically concatenating the matrices $\{\mathbf{H}_v\}$, $v = 1, \dots, V$. As it is suggested in [26], (17) has a closed-form solution:

$$\mathbf{E}_i^{t+1} = \begin{cases} \frac{\|\mathbf{H}_i^t\|_2^{-\frac{1}{\tau^t}}}{\|\mathbf{H}_i^t\|_2} \mathbf{H}_i^t, & \text{if } \frac{1}{\tau^t} < \|\mathbf{H}_i^t\|_2 \\ 0, & \text{otherwise} \end{cases} \quad (18)$$

where \mathbf{H}_i^t and \mathbf{E}_i^{t+1} denote the i -th column of \mathbf{H}^t and \mathbf{E}^{t+1} , respectively.

Solving M-subproblem: The optimization subproblem with respect to \mathbf{M} is:

$$\begin{aligned} \min_{\mathbf{M}} \quad & \sum_{v=1}^V \mu \operatorname{tr}(\mathbf{S}_v^{t+1\top} \mathbf{L} \mathbf{S}_v^{t+1}) + \lambda \|\mathbf{M}\|_{\mathbf{F}}^2 \\ \text{s. t.} \quad & \mathbf{M}^{\top} \mathbf{1} = \mathbf{1}, \mathbf{0} \leq \mathbf{M} \leq \mathbf{1}. \end{aligned} \quad (19)$$

According to (3) and (4), (19) can be divided into i subproblems:

$$\begin{aligned} \min_{\mathbf{M}_i} \quad & \sum_{j=1}^N \sum_{v=1}^V \frac{\mu}{2} \|(\mathbf{S}_i^{t+1})_v - (\mathbf{S}_j^{t+1})_v\|_2^2 m_{i,j} + \lambda \sum_{j=1}^N m_{i,j}^2 \\ \text{s. t.} \quad & \mathbf{M}_i^{\top} \mathbf{1} = 1, \mathbf{0} \leq \mathbf{M}_i \leq \mathbf{1}. \end{aligned} \quad (20)$$

where \mathbf{M}_i is the i -th column of matrix \mathbf{M} and $(\mathbf{S}_i)_v$ is the i -th column of matrix \mathbf{S}_v . Following [7, 17] that apply the adaptive neighbor scheme to keep K largest values constant in \mathbf{M}_i and the rest become zero, each subproblem has the solution:

$$\begin{cases} m_{ij}^{l+1} = \frac{p_{i,K+1} - p_{ij}}{K p_{i,K+1} - \sum_{k=1}^K p_{i,k}}, j \leq K \\ m_{ij}^{l+1} = 0, j > K. \end{cases} \quad (21)$$

where $p_{i,j} = \sum_{v=1}^V \|(\mathbf{s}_i^{l+1})_v - (\mathbf{s}_j^{l+1})_v\|_2^2$ and $\mathbf{p}_i \in \mathbb{R}^{N \times 1}$.

Updating \mathcal{W} , \mathcal{Y} and τ : By keeping other variables, i.e., \mathcal{Z} , \mathcal{S} and \mathbf{E} are fixed, the Lagrangian multipliers \mathcal{W} , \mathcal{Y} and the penalty parameter τ are updated as follows:

$$\begin{aligned} \mathbf{W}_v^{t+1} &= \mathbf{W}_v^t + \tau^t (\mathbf{X}_v - \mathbf{X}_v \mathbf{S}_v^{t+1} - \mathbf{E}_v^{t+1}), \\ \mathcal{Y}^{t+1} &= \mathcal{Y}^t + \tau^t (\mathcal{Z}^{t+1} - \mathcal{S}^{t+1}), \\ \tau^{t+1} &= \min \{ \beta \tau^t, \tau_{\max} \}, \end{aligned} \quad (22)$$

where $\beta > 1$ is utilized to accelerate the convergence, and τ_{\max} is the predefined maximum value of τ . The affinity matrix \mathbf{M} , which will be put into spectral clustering algorithm to yield the final clustering results, can be calculated by $\mathbf{M} = 1/V \sum_{v=1}^V (|\mathbf{Z}_v| + |\mathbf{Z}_v^{\top}|)$.

4.3 Computational Complexity

To analyze the computation complexity of TOMD-MVC, we assume that $R = R_1 = \dots = R_4 = D_1 = \dots = D_6$ for convenience of analysis. At each iteration, it takes $\mathcal{O}(IN_1N_2N_3VR^4)$ to update the reshaped tensor $\mathcal{Z} \in \mathbb{R}^{N_1 \times N_2 \times N_3 \times V}$, where I denotes number of iterations of TOMD-ALS. For \mathcal{S} -subproblem, we need $\mathcal{O}(VN^3)$ to compute its closed-form. Updating \mathbf{E} and \mathbf{M} cost $\mathcal{O}(VN^2)$ and $\mathcal{O}(N^2)$, respectively. Therefore, the computation in each iteration is $\mathcal{O}(V(IN_1N_2N_3R^4 + N^3 + N^2) + N^2)$.

In addition, after we get the affinity matrix, we adopt the spectral clustering method to obtain the final memberships of data. Considering the spectral clustering's computational complexity is $\mathcal{O}(N^3)$ [45], the overall complexity is $\mathcal{O}(TV(IN_1N_2N_3R^4 + N^3 + N^2) + LN^2 + N^3)$, where T is the iteration number of TOMD-MVC.

Algorithm 2 TOMD for low rank multi-view clustering

Input: Multi-view data $\{\mathbf{X}_v\}, v = 1, \dots, V$, μ and K , $\text{iter}_{\max} = 150$, and N_1, N_2, N_3, V .

Initialization: $\mathcal{S}, \mathcal{Z}, \mathbf{E}, \mathbf{M}, \mathcal{W}, \mathcal{Y}$ initialized to $\mathbf{0}$, $\tau = 1$, $\beta = 1.5$, $\text{tol} = 10^{-7}$, iteration $t = 1$.

while $t \leq \text{iter}_{\max}$ **do**

$\tilde{\mathcal{S}}^t = \Phi((\mathcal{S}^t - \frac{\Pi^t}{\tau}), [N_1, N_2, N_3, V]);$

 Obtain $\{\tilde{\mathcal{G}}^{(n)}\}_{n=1}^5, \{\tilde{\mathbf{U}}^{(n)}\}_{n=1}^4$ by TOMD-ALS and update \mathcal{Z}^{t+1} by (14);

for $v = 1 : V$ **do**

 Update \mathbf{S}_v^{t+1} ;

end for

 Update \mathbf{E}^{t+1} and \mathbf{M}^{t+1} by (18) and (21), respectively;

 Update $\mathcal{W}^{t+1}, \mathcal{Y}^{t+1}$ and τ^{t+1} by (22);

 Check convergence conditions:

$\max(\|\mathbf{X}_v - \mathbf{X}_v \mathbf{S}_v^{t+1} - \mathbf{E}_v^{t+1}\|_{\infty}, \|\mathcal{Z}^{t+1} - \mathcal{S}^{t+1}\|_{\infty}) \leq \text{tol};$

$t=t+1$;

end while

Output: Affinity matrix \mathbf{M}^{t+1} .

5 Experiments

In this section, image reconstruction experiments have been employed to indicate our proposed tensor network’s advantages in depicting low-rank properties. The clustering performance of our proposed method has also been demonstrated over six multi-view datasets.

5.1 Low-Rank Analysis

To illustrate the superiority of our proposed tensor network, we conduct the image reconstruction experiments on several real word images¹: ”House”, ”Peppers”, ”Airplane (F-16)”, ”Sailboat on lake”, and ”Airplane”. Since the TOMD has been utilized for 4th-order tensors, the gray forms of these images are further transformed into $16 \times 16 \times 16 \times 16$ tensors.

In this section, the tensors are performed by Tucker-ALS, Tucker and tensor ring decomposition ALS (TuTR-ALS), O-Minus-ALS (Ominus-ALS) and TOMD-ALS algorithms with the same Relative standard error (RSE) [52]. Beyond that, the storage costs of the different decomposition have been calculated and presented in Table 2. In addition to the time needed for pre-processing the images, reconstructing the images, and calculating the storage costs, the running time in our experiments only contains the main body in decomposition, which is also illustrated in Table 2. Considering that the speed of the iterative algorithm primarily affects the running time of those methods, we set the number of iterations for all methods to 500 in our experiment.

¹<http://sipi.usc.edu/database/database.php?volume=misc>

As results shown in Table 2, under the same conditions, we can conclude that the running time of TOMD is in the middle, but it has the lowest storage cost and can better exploit the low rank information compared to the other decompositions.

Table 2: Comparison results about Tucker-ALS, TuTR-ALS, Ominus-ALS and TOMD-ALS algorithms based image reconstruction experiments, and the values under the datasets’ name are the predefined RSE.

Dataset	Method	Time(s)	Storage Cost
House (0.12)	Tucker-ALS	17.10	2473
	TuTR-ALS	20.21	1872
	Ominus-ALS	11.34	1545
	TOMD-ALS	17.22	1220
Peppers (0.12)	Tucker-ALS	80.74	11904
	TuTR-ALS	40.51	4898
	Ominus-ALS	45.93	4825
	TOMD-ALS	47.48	3072
F-16 (0.12)	Tucker-ALS	55.66	4608
	TuTR-ALS	29.12	2340
	Ominus-ALS	12.41	1801
	TOMD-ALS	17.22	1484
Sailboat (0.12)	Tucker-ALS	85.83	10640
	TuTR-ALS	45.03	5820
	Ominus-ALS	51.66	6361
	TOMD-ALS	47.62	4894
Airplane (0.06)	Tucker-ALS	11.30	2849
	TuTR-ALS	30.22	2080
	Ominus-ALS	12.49	2507
	TOMD-ALS	26.81	1516

5.2 Experimental Settings For Multi-view Clustering

5.2.1 Datasets

The performance of TOMD-MVC has been investigated over six multi-view datasets, Yale², MSRCV1³, ExtendYaleB [44], ORL⁴, Reuters⁵ and Handwritten [6], and their statistic information has been summarized in Table 3.

²<http://cvc.cs.yale.edu/cvc/projects/yalefaces/yalefaces.html>

³<http://research.microsoft.com/en-us/projects/objectclassrecognition/>

⁴<http://www.uk.research.att.com/facedatabase.html>

⁵<http://lig-membres.imag.fr/grimal/data.html>

Table 3: Statistics of different datasets.

Datasets	Feature(C_1, \dots, C_v)	Samples(N)	Views(V)	Clusters	Objective	(N_1, N_2, N_3, V)
Yale	(4096,3304,6750)	165	3	15	Face	(165,15,11,3)
MSRCV1	(1302,48,512,100,256,210)	210	6	7	Object	(210,15,14,6)
ExtendYaleB	(2500,3304,6750)	650	3	10	Face	(50,13,650,3)
ORL	(4096,3304,6750)	400	3	40	Face	(400,20,20,3)
Reuters	(4819,4810,4892,4858,4777)	1200	5	6	Text	(1200,20,60,5)
Handwritten	(240,76,216,47,64,6)	2000	6	10	Digit	(200,10,200,60)

5.2.2 Competitors

We compare our TOMD-MVC model with six matrix based methods, GMC [43], GFSC [18], LMSC [55], SFMC [24], EOMSC-CA [29], COMSC [28], and six multi-view clustering methods, LTMSC [53], t-SVD-MS [48], ETLMSC [45], UGLTL [46], HLR-M²VC [49], TBGL [47], to verify its superiority.

5.2.3 Evaluation Metrics

In our experiments, six commonly used metrics are applied to quantitatively evaluate the clustering performance, namely F-score, precision (P), recall (R), normalized mutual information (NMI), adjusted rand index (AR), and accuracy (ACC). In addition, the higher values of these metrics indicate better clustering performance. Further detailed information please refer to [14, 25, 39, 56, 60].

5.3 Clustering Performance Comparison

5.3.1 Compared with state-of-the-art methods

All detailed clustering results on six data sets are presented in Table 4-9. Since the different initializations may lead to different results, we run 10 trials for each experiment and present their average performance with standard deviations, i.e., mean(standard deviation). The best results are highlighted in **boldface** and the second-best results are underlined.

LTMSC, t-SVD-MS [48], ETLMSC, UGLTL, HLR-M²VC, and TBGL are all tensor-based methods, whose clustering performance is almost higher than matrix based methods. Therefore, employing the tensor based low rank constraints on self-representation tensor is a better way to capture the higher-order correlations. Nevertheless, our proposed TOMD-MVC can still achieve the best results among these tensor-based methods under all six evaluation metrics. Specifically, the results of our proposed model on Yale, ORL and Reuters data sets, are 1.5%, 1.13%, 6.57% higher than the second-best method, respectively. Especially on the ExtendYaleB dataset, the improvement of TOMD-MVC is at least 30% higher than the second-best performance of t-SVD-MS. Based on this, we can demonstrate the superiority of our proposed tensor network in low rank multi-view clustering.

Table 4: Clustering results on Yale dataset. For TOMD-MVC, we set $K = 10$ and $\mu = 1$.

Method	F-score	Precision	Recall	NMI	AR	ACC
GMC	0.446(0.000)	0.378(0.000)	0.544(0.000)	0.668(0.000)	0.403(0.000)	0.618(0.000)
GFSC	0.433(0.028)	0.384(0.040)	0.497(0.016)	0.647(0.015)	0.391(0.032)	0.621(0.029)
LMSC	0.519(0.003)	0.475(0.006)	0.572(0.000)	0.717(0.002)	0.484(0.004)	0.679(0.007)
SFMC	0.480(0.000)	0.438(0.000)	0.532(0.000)	0.663(0.000)	0.443(0.000)	0.618(0.000)
EOMSC-CA	0.469(0.000)	0.418(0.000)	0.533(0.000)	0.654(0.000)	0.430(0.000)	0.648(0.000)
LTMSC	0.620(0.009)	0.599(0.011)	0.643(0.006)	0.764(0.006)	0.594(0.009)	0.736(0.004)
t-SVD-MSC	0.902(0.066)	0.891(0.075)	0.915(0.058)	0.946(0.036)	0.896(0.071)	0.934(0.053)
ETLMSC	0.542(0.055)	0.509(0.053)	0.580(0.061)	0.706(0.043)	0.510(0.059)	0.654(0.044)
UGLTL	0.867(0.047)	0.852(0.057)	0.883(0.039)	0.931(0.023)	0.858(0.050)	0.912(0.041)
HLR-M ² VC	0.695(0.010)	0.673(0.011)	0.718(0.010)	0.817(0.006)	0.674(0.011)	0.772(0.012)
COMSC	0.627(0.000)	0.607(0.000)	0.953(0.000)	0.762(0.000)	0.602(0.000)	0.739(0.000)
TBGL	0.587(0.000)	0.556(0.000)	0.623(0.000)	0.739(0.000)	0.559(0.000)	0.703(0.000)
TOMD-MVC	0.916(0.013)	0.914(0.014)	0.918(0.013)	0.949(0.008)	0.910(0.014)	0.959(0.006)

Table 5: Clustering results on MSRCV1 dataset. For TOMD-MVC, we set $K = 5$ and $\mu = 50$.

Method	F-score	Precision	Recall	NMI	AR	ACC
GMC	0.824(0.000)	0.812(0.000)	0.837(0.000)	0.846(0.000)	0.795(0.000)	0.910(0.000)
GFSC	0.609(0.050)	0.581(0.065)	0.642(0.031)	0.661(0.042)	0.542(0.062)	0.730(0.061)
LMSC	0.656(0.081)	0.646(0.081)	0.667(0.080)	0.677(0.065)	0.600(0.094)	0.783(0.086)
SFMC	0.763(0.000)	0.701(0.000)	0.836(0.000)	0.790(0.000)	0.720(0.000)	0.838(0.000)
EOMSC-CA	0.813(0.000)	0.787(0.000)	0.840(0.000)	0.837(0.000)	0.781(0.000)	0.876(0.000)
LTMSC	0.727(0.001)	0.714(0.001)	0.742(0.000)	0.750(0.000)	0.682(0.001)	0.829(0.000)
t-SVD-MSC	0.962(0.000)	0.961(0.000)	0.963(0.000)	0.960(0.000)	0.955(0.000)	0.981(0.000)
ETLMSC	0.934(0.079)	0.924(0.099)	0.946(0.056)	0.946(0.055)	0.923(0.092)	0.950(0.077)
UGLTL	1.000(0.000)	1.000(0.000)	1.000(0.000)	1.000(0.000)	1.000(0.000)	1.000(0.000)
HLR-M ² VC	0.990(0.000)	0.990(0.000)	0.990(0.000)	0.989(0.000)	0.989(0.000)	0.995(0.000)
COMSC	0.861(0.000)	0.856(0.000)	0.961(0.000)	0.863(0.000)	0.838(0.000)	0.929(0.000)
TBGL	1.000(0.000)	1.000(0.000)	1.000(0.000)	1.000(0.000)	1.000(0.000)	1.000(0.000)
TOMD-MVC	1.000(0.000)	1.000(0.000)	1.000(0.000)	1.000(0.000)	1.000(0.000)	1.000(0.000)

Table 6: Clustering results on ExtendYaleB dataset. For TOMD-MVC, we set $K = 15$ and $\mu = 50$.

Method	F-score	Precision	Recall	NMI	AR	ACC
GMC	0.256(0.000)	0.201(0.000)	0.351(0.000)	0.405(0.000)	0.149(0.000)	0.386(0.000)
GFSC	0.204(0.006)	0.161(0.004)	0.282(0.024)	0.327(0.023)	0.090(0.005)	0.348(0.025)
LMSC	0.352(0.001)	0.309(0.001)	0.410(0.001)	0.513(0.001)	0.270(0.001)	0.530(0.001)
SFMC	0.290(0.000)	0.197(0.000)	0.551(0.000)	0.494(0.000)	0.170(0.000)	0.509(0.000)
EOMSC-CA	0.202(0.000)	0.169(0.000)	0.252(0.000)	0.250(0.000)	0.095(0.000)	0.289(0.000)
LTMSC	0.323(0.005)	0.296(0.006)	0.355(0.004)	0.456(0.004)	0.242(0.006)	0.455(0.002)
t-SVD-MSC	0.483(0.005)	0.456(0.007)	0.513(0.004)	0.618(0.003)	0.422(0.006)	0.577(0.001)
ETLMSC	0.262(0.017)	0.257(0.017)	0.590(0.008)	0.307(0.021)	0.179(0.019)	0.325(0.011)
UGLTL	0.406(0.038)	0.395(0.036)	0.417(0.041)	0.503(0.044)	0.339(0.042)	0.463(0.037)
HLR-M ² VC	0.575(0.000)	0.553(0.000)	0.599(0.000)	0.706(0.000)	0.527(0.000)	0.673(0.000)
COMSC	0.453(0.000)	0.414(0.000)	0.881(0.000)	0.596(0.000)	0.387(0.000)	0.616(0.000)
TBGL	0.230(0.000)	0.156(0.000)	0.437(0.000)	0.382(0.000)	0.100(0.000)	0.403(0.000)
TOMD-MVC	0.981(0.001)	0.981(0.001)	0.981(0.001)	0.982(0.001)	0.979(0.001)	0.990(0.001)

Table 7: Clustering results on ORL dataset. For TOMD-MVC, we set $K = 10$ and $\mu = 30$.

Method	F-score	Precision	Recall	NMI	AR	ACC
GMC	0.368(0.000)	0.239(0.000)	0.805(0.000)	0.861(0.000)	0.345(0.000)	0.660(0.000)
GFSC	0.501(0.053)	0.413(0.063)	0.644(0.035)	0.828(0.019)	0.487(0.055)	0.636(0.046)
LMSC	0.776(0.016)	0.717(0.024)	0.847(0.013)	0.932(0.005)	0.771(0.017)	0.823(0.016)
SFMC	0.702(0.000)	0.586(0.000)	0.876(0.000)	0.908(0.000)	0.694(0.000)	0.775(0.000)
EOMSC-CA	0.461(0.000)	0.365(0.000)	0.627(0.000)	0.791(0.000)	0.446(0.000)	0.613(0.000)
LTMSC	0.766(0.025)	0.725(0.028)	0.813(0.023)	0.920(0.010)	0.760(0.026)	0.817(0.021)
t-SVD-MSC	0.987(0.017)	0.979(0.027)	0.996(0.006)	0.997(0.003)	0.987(0.017)	0.987(0.017)
ETLMSC	0.928(0.027)	0.894(0.036)	0.966(0.019)	0.982(0.009)	0.927(0.028)	0.929(0.025)
UGLTL	0.948(0.017)	0.932(0.022)	0.965(0.013)	0.985(0.005)	0.947(0.017)	0.954(0.016)
HLR-M ² VC	0.991(0.015)	0.984(0.026)	0.997(0.005)	0.998(0.003)	0.990(0.016)	0.991(0.015)
COMSC	0.770(0.000)	0.730(0.000)	0.989(0.000)	0.913(0.000)	0.764(0.000)	0.835(0.000)
TBGL	0.611(0.000)	0.470(0.000)	0.871(0.000)	0.895(0.000)	0.599(0.000)	0.848(0.000)
TOMD-MVC	1.000(0.000)	1.000(0.000)	1.000(0.000)	1.000(0.000)	1.000(0.000)	1.000(0.000)

Table 8: Clustering results on Reuters dataset. For TOMD-MVC, we set $K = 20$ and $\mu = 50$.

Method	F-score	Precision	Recall	NMI	AR	ACC
GMC	0.283(0.000)	0.167(0.000)	0.927(0.000)	0.075(0.000)	0.003(0.000)	0.187(0.000)
GFSC	0.328(0.010)	0.254(0.020)	0.475(0.055)	0.226(0.024)	0.143(0.026)	0.375(0.045)
LMSC	0.407(0.000)	0.374(0.000)	0.447(0.000)	0.342(0.000)	0.276(0.000)	0.562(0.000)
SFMC	0.284(0.000)	0.166(0.000)	0.966(0.000)	0.019(0.000)	0.001(0.000)	0.182(0.000)
EOMSC-CA	0.312(0.000)	0.291(0.000)	0.335(0.000)	0.223(0.000)	0.163(0.000)	0.427(0.000)
LTMSC	0.304(0.000)	0.253(0.000)	0.380(0.000)	0.196(0.001)	0.130(0.000)	0.382(0.001)
t-SVD-MSC	0.904(0.000)	0.902(0.000)	0.907(0.000)	0.885(0.000)	0.885(0.000)	0.950(0.000)
ETLMSC	0.898(0.114)	0.891(0.128)	0.907(0.098)	0.896(0.087)	0.877(0.138)	0.920(0.118)
UGLTL	0.934(0.000)	0.933(0.000)	0.934(0.000)	0.914(0.000)	0.920(0.000)	0.966(0.000)
HLR-M ² VC	0.714(0.001)	0.704(0.001)	0.724(0.001)	0.708(0.001)	0.656(0.001)	0.831(0.001)
COMSC	0.407(0.000)	0.349(0.000)	0.764(0.000)	0.330(0.000)	0.264(0.000)	0.547(0.000)
TBGL	0.284(0.000)	0.167(0.000)	0.951(0.000)	0.029(0.000)	0.002(0.000)	0.179(0.000)
TOMD-MVC	0.964(0.013)	0.963(0.014)	0.966(0.012)	0.957(0.016)	0.957(0.016)	0.981(0.007)

Table 9: Clustering results on Handwritten dataset. For TOMD-MVC, we set $K = 20$ and $\mu = 40$.

Method	F-score	Precision	Recall	NMI	AR	ACC
GMC	0.854(0.000)	0.793(0.000)	0.925(0.000)	0.910(0.000)	0.836(0.000)	0.857(0.000)
GFSC	0.630(0.049)	0.573(0.052)	0.700(0.054)	0.715(0.026)	0.584(0.056)	0.714(0.053)
LMSC	0.818(0.001)	0.815(0.001)	0.820(0.001)	0.816(0.001)	0.797(0.001)	0.901(0.000)
SFMC	0.868(0.000)	0.820(0.000)	0.920(0.000)	0.892(0.000)	0.852(0.000)	0.881(0.000)
EOMSC-CA	0.710(0.000)	0.613(0.000)	0.842(0.000)	0.775(0.000)	0.672(0.000)	0.725(0.000)
LTMSC	0.818(0.016)	0.815(0.016)	0.821(0.015)	0.833(0.010)	0.797(0.017)	0.896(0.012)
t-SVD-MSC	0.999(0.000)	0.999(0.000)	0.999(0.000)	0.999(0.000)	0.999(0.000)	1.000(0.000)
ETLMSC	0.919(0.071)	0.880(0.107)	0.965(0.027)	0.964(0.030)	0.909(0.080)	0.902(0.089)
UGLTL	1.000(0.000)	1.000(0.000)	1.000(0.000)	1.000(0.000)	1.000(0.000)	1.000(0.000)
HLR-M ² VC	1.000(0.000)	1.000(0.000)	1.000(0.000)	1.000(0.000)	1.000(0.000)	1.000(0.000)
COMSC	0.885(0.000)	0.883(0.000)	0.977(0.000)	0.881(0.000)	0.872(0.000)	0.940(0.000)
TBGL	0.849(0.000)	0.792(0.000)	0.914(0.000)	0.894(0.000)	0.831(0.000)	0.843(0.000)
TOMD-MVC	1.000(0.000)	1.000(0.000)	1.000(0.000)	1.000(0.000)	1.000(0.000)	1.000(0.000)

5.3.2 Compared with Tucker decomposition based methods

In this section, we implement a number of experiments to evaluate the influence of applying higher-order form and O-minus structure on self-representation tensor \mathcal{Z} in multi-view clustering. The primary procedure of clustering algorithm are same except for updating tensor \mathcal{Z} . Specifically, with 4-Dimensional Tucker decomposition based multi-view clustering model (4DT-MVC), we reshape \mathcal{Z} into a 4th-order tensor and employs Tucker decomposition to capture its low-rank information while solving the problem with respect to \mathcal{Z} . As for the 3-Dimensional Tucker decomposition based MVC method (3DT-MVC), the representation tensor maintained 3rd-order. The average results after 10 runs of each experiment with six metrics are all presented in Table 10.

As results show, the improvements of 4DT-MVC are around 29.50%, 10.57%, 6.87%, 8.09%, 2.67% about the average of six metrics over 3DT-MVC on Yale, MSRCV1, ExtendYaleB, ORL and Handwritten datasets, respectively. Especially for the Reuters data set, 4DT-MVC is more than twice as much as 3DT-MVC. The main reason may be that more low-rank information can be discovered in high-dimensional space. In addition, TOMD has a further 7.16%, 2.76%, 0.56%, 0.42%, 5.21%, 2.92% development over 4DT-MVC on the same datasets, demonstrating the superiority of our proposed tensor network TOMD.

Table 10: Clustering results on six datasets obtained by different tensor decomposition constraints.

Datasets	Method	F-score	Precision	Recall	NMI	AR	ACC
Yale	3DT-MVC	0.635	0.611	0.660	0.781	0.610	0.738
	4DT-MVC	0.842	0.825	0.861	0.913	0.832	0.927
	TOMD-MVC	0.916	0.914	0.918	0.949	0.910	0.959
MSRCV1	3DT-MVC	0.879	0.866	0.892	0.869	0.840	0.943
	4DT-MVC	0.972	0.971	0.973	0.971	0.967	0.986
	TOMD-MVC	1.000	1.000	1.000	1.000	1.000	1.000
ExtendYaleB	3DT-MVC	0.909	0.908	0.911	0.905	0.899	0.954
	4DT-MVC	0.975	0.974	0.975	0.976	0.973	0.988
	TOMD-MVC	0.981	0.981	0.981	0.982	0.979	0.990
ORL	3DT-MVC	0.908	0.888	0.928	0.970	0.905	0.933
	4DT-MVC	0.995	0.994	0.995	0.998	0.995	0.998
	TOMD-MVC	1.000	1.000	1.000	1.000	1.000	1.000
Reuters	3DT-MVC	0.445	0.377	0.543	0.441	0.310	0.584
	4DT-MVC	0.922	0.921	0.924	0.917	0.907	0.957
	TOMD-MVC	0.964	0.963	0.966	0.957	0.957	0.981
Handwritten	3DT-MVC	0.945	0.944	0.945	0.934	0.939	0.972
	4DT-MVC	0.971	0.971	0.971	0.963	0.968	0.986
	TOMD-MVC	1.000	1.000	1.000	1.000	1.000	1.000

5.4 Model Discussion

5.4.1 Representation Visualization

Fig. 2 visualizes the affinity matrices learned by different clustering methods. Due to the limitations of space, we only present the results of LMSC, t-SVD-MSVC and TOMD-MVC on ORL dataset. Compared with the other three methods, our proposed TOMD-MVC is much better as its visualization matrix gives a more clear block-diagonal structure on ORL dataset.

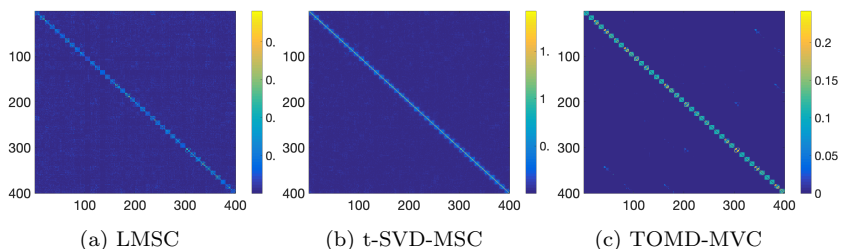


Figure 2: Comparison of affinity matrix on ORL dataset by LMSC, t-SVD-MSVC and TOMD-MVC.

5.4.2 Convergence

In Fig. 3, we respectively plot the convergence curves of 3DT-MVC, 4DT-MVC and TOMD-MVC methods, where the X-axis is the number of iterations, and Y-axis is the value of Reconstruction Error $= (1/V) \sum_{v=1}^V \|\mathbf{X}_v - \mathbf{X}_v \mathbf{S}_v - \mathbf{E}_v\|_\infty$ and Match Error $= (1/V) \sum_{v=1}^V \|\mathbf{Z}_v - \mathbf{S}_v\|_\infty$. As the results show, the 3DT-MVC converges faster on the MSRCV1 dataset. However, its clustering performance does not perform well compared to the 4DT-MVC and TOMD-MVC. The convergence speed of the TOMD algorithm is similar to that of 4DT-MVC as presented in Fig. 3. Nonetheless, our proposed method has a further 2.76% development over 4DT-MVC on MSRCV1 as illustrated in Table 10. Empirically, the number of optimization iteration is usually located within the range of (100, 150).

5.4.3 Parameter Sensitivity Analysis

As suggested in [7], the parameter λ can be determined by the number of adaptive neighbors K . Therefore, there are three free parameters in our model: balanced parameter μ , the number of adaptive neighbors K and tensor ranks $(R_1, \dots, R_4, D_1, \dots, D_6)$. Due to the limitations of the paper, we only show the results of ACC and NMI on Yale dataset by the combination of different μ and K in Fig. 4. We can see that the performance of TOMD-MVC is relatively stable when $\mu = [5, 50]$ and $K = [5, 15]$ on Yale dataset. Besides, the evaluation results on Yale dataset have been presented in Table 11 with different rank

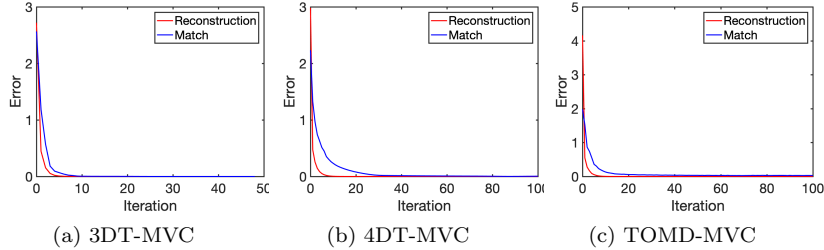


Figure 3: The convergence curves on MSRCV1 dataset.

tuning. The results show that TOMD-MVC can achieve promising performance while the pre-defined ranks are set as $(30, 15, 11, V, 4, 4, 4, 4, 4, 4)$, where V is the number of views.

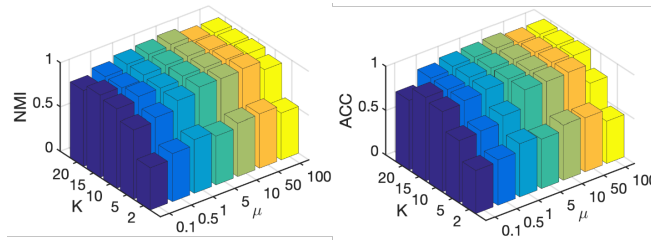


Figure 4: Parameters tuning (μ and K) in terms of ACC and NMI on MSRCV1.

Table 11: Clustering results of TOMD-MVC with different ranks on Yale dataset.

$(R_1, \dots, R_4, D_1, \dots, D_6)$	F-score	Precision	Recall	NMI	AR	ACC
(10, 5, 5, V , 2, 2, 2, 2, 2, 2)	0.626(0.018)	0.595(0.016)	0.660(0.021)	0.812(0.010)	0.600(0.020)	0.723(0.029)
(10, 10, 5, V , 2, 2, 2, 2, 2, 2)	0.624(0.019)	0.594(0.016)	0.657(0.023)	0.808(0.012)	0.598(0.020)	0.730(0.020)
(10, 5, 10, V , 2, 2, 2, 2, 2, 2)	0.623(0.008)	0.583(0.007)	0.670(0.011)	0.813(0.005)	0.597(0.009)	0.707(0.020)
(20, 5, 5, V , 2, 2, 2, 2, 2, 2)	0.630(0.017)	0.598(0.015)	0.666(0.020)	0.813(0.010)	0.605(0.019)	0.724(0.034)
(10, 5, 5, V , 4, 4, 4, 4, 4, 4)	0.490(0.032)	0.464(0.035)	0.520(0.030)	0.711(0.021)	0.455(0.035)	0.652(0.034)
(20, 10, 10, V , 4, 4, 4, 4, 4, 4)	0.844(0.022)	0.835(0.022)	0.852(0.022)	0.910(0.014)	0.833(0.023)	0.921(0.012)
(20, 15, 10, V , 4, 4, 4, 4, 4, 4)	0.843(0.012)	0.833(0.015)	0.854(0.010)	0.909(0.006)	0.833(0.013)	0.922(0.006)
(20, 10, 11, V , 4, 4, 4, 4, 4, 4)	0.887(0.015)	0.884(0.015)	0.891(0.015)	0.932(0.010)	0.880(0.016)	0.944(0.008)
(30, 10, 10, V , 4, 4, 4, 4, 4, 4)	0.858(0.012)	0.849(0.014)	0.866(0.010)	0.918(0.006)	0.848(0.013)	0.929(0.006)
(30, 15, 11, V , 6, 6, 6, 6, 6, 6)	0.637(0.007)	0.613(0.010)	0.663(0.005)	0.782(0.004)	0.613(0.008)	0.738(0.006)
(30, 15, 11, V , 4, 4, 4, 4, 4, 4)	0.916(0.013)	0.914(0.014)	0.918(0.013)	0.949(0.008)	0.910(0.014)	0.959(0.006)
(40, 15, 11, V , 4, 4, 4, 4, 4, 4)	0.896(0.008)	0.892(0.009)	0.899(0.008)	0.937(0.005)	0.889(0.009)	0.948(0.004)

6 Conclusion

In this paper, we propose a novel tensor network called TOMD to considerably capture the low-rank property of representation tensor and fully explore the la-

tent correlations across different views in clustering. In addition, we drive a detailed algorithm to solve the optimization problem. Accordingly, TOMD-MVC has been developed and its superiority performance has been demonstrated by extensive experimental results on six real-world datasets.

Acknowledgment

This work was supported by the National Natural Science Foundation of China (NSFC) under Grant 62171088, Grant 6220106011 and Grant U19A2052.

References

- [1] Tülay Adalı, Furkan Kantar, Mohammad Abu Baker Siddique Akhonda, Stephen Strother, Vince D Calhoun, and Evrim Acar. Reproducibility in matrix and tensor decompositions: Focus on model match, interpretability, and uniqueness. *IEEE Signal Processing Magazine*, 39(4):8–24, 2022.
- [2] Johann A Bengua, Ho N Phien, Hoang Duong Tuan, and Minh N Do. Efficient tensor completion for color image and video recovery: Low-rank tensor train. *IEEE Transactions on Image Processing*, 26(5):2466–2479, 2017.
- [3] M Billó, F Fucito, GP Korchemsky, A Lerda, and JF Morales. Two-point correlators in non-conformal $\mathcal{N}=2$ gauge theories. *Journal of High Energy Physics*, 2019(5):1–56, 2019.
- [4] J Douglas Carroll and Jih-Jie Chang. Analysis of individual differences in multidimensional scaling via an n-way generalization of “eckart-young” decomposition. *Psychometrika*, 35(3):283–319, 1970.
- [5] Hongyang Chen, Fauzia Ahmad, Sergiy Vorobyov, and Fatih Porikli. Tensor decompositions in wireless communications and mimo radar. *IEEE Journal of Selected Topics in Signal Processing*, 15(3):438–453, 2021.
- [6] Peng Chen, Liang Liu, Zhengrui Ma, and Zhao Kang. Smoothed multi-view subspace clustering. In *International Conference on Neural Computing for Advanced Applications*, pages 128–140. Springer, 2021.
- [7] Yongyong Chen, Xiaolin Xiao, Chong Peng, Guangming Lu, and Yicong Zhou. Low-rank tensor graph learning for multi-view subspace clustering. *IEEE Transactions on Circuits and Systems for Video Technology*, 2021.
- [8] Zefeng Chen, Guoxu Zhou, and Qibin Zhao. Hierarchical factorization strategy for high-order tensor and application for data completion. *IEEE Signal Processing Letters*, 2021.

- [9] Andrzej Cichocki, Namgil Lee, Ivan V Oseledets, A-H Phan, Qibin Zhao, and D Mandic. Low-rank tensor networks for dimensionality reduction and large-scale optimization problems: Perspectives and challenges part 1. *Foundations and Trends in Machine Learning*, 9(4-5):249–429, 2016.
- [10] Lanlan Feng, Ce Zhu, and Yipeng Liu. Multi-mode tensor singular value decomposition for low-rank image recovery. In *International Conference on Image and Graphics*, pages 238–249. Springer, 2021.
- [11] John A Hartigan and Manchek A Wong. Algorithm as 136: A k-means clustering algorithm. *Journal of The Royal Statistical Society. Series C (Applied Statistics)*, 28(1):100–108, 1979.
- [12] Lifang He, Chun-Ta Lu, Yong Chen, Jiawei Zhang, Linlin Shen, S Yu Philip, and Fei Wang. A self-organizing tensor architecture for multi-view clustering. In *2018 IEEE International Conference on Data Mining (ICDM)*, pages 1007–1012. IEEE, 2018.
- [13] Chenping Hou, Feiping Nie, Hong Tao, and Dongyun Yi. Multi-view unsupervised feature selection with adaptive similarity and view weight. *IEEE Transactions on Knowledge and Data Engineering*, 29(9):1998–2011, 2017.
- [14] Dong Huang, Chang-Dong Wang, Jian-Sheng Wu, Jian-Huang Lai, and Chee-Keong Kwoh. Ultra-scalable spectral clustering and ensemble clustering. *IEEE Transactions on Knowledge and Data Engineering*, 32(6):1212–1226, 2019.
- [15] Yuwang Ji, Qiang Wang, Xuan Li, and Jie Liu. A survey on tensor techniques and applications in machine learning. *IEEE Access*, 7:162950–162990, 2019.
- [16] Rohit Kumar Kaliyar, Anurag Goswami, and Pratik Narang. Deepfake: improving fake news detection using tensor decomposition-based deep neural network. *The Journal of Supercomputing*, 77(2):1015–1037, 2021.
- [17] Zhao Kang, Haiqi Pan, Steven CH Hoi, and Zenglin Xu. Robust graph learning from noisy data. *IEEE Transactions on Cybernetics*, 50(5):1833–1843, 2019.
- [18] Zhao Kang, Guoxin Shi, Shudong Huang, Wenyu Chen, Xiaorong Pu, Joey Tianyi Zhou, and Zenglin Xu. Multi-graph fusion for multi-view spectral clustering. *Knowledge-Based Systems*, 189:105102, 2020.
- [19] Henk AL Kiers. Towards a standardized notation and terminology in multiway analysis. *Journal of Chemometrics: A Journal of the Chemometrics Society*, 14(3):105–122, 2000.
- [20] Misha E Kilmer and Carla D Martin. Factorization strategies for third-order tensors. *Linear Algebra and its Applications*, 435(3):641–658, 2011.

- [21] Misha E Kilmer, Carla D Martin, and Lisa Perrone. A third-order generalization of the matrix svd as a product of third-order tensors. *Tufts University, Department of Computer Science, Tech. Rep. TR-2008-4*, 2008.
- [22] Tamara G Kolda and Brett W Bader. Tensor decompositions and applications. *SIAM Review*, 51(3):455–500, 2009.
- [23] Pieter M Kroonenberg and Jan De Leeuw. Principal component analysis of three-mode data by means of alternating least squares algorithms. *Psychometrika*, 45(1):69–97, 1980.
- [24] Xuelong Li, Han Zhang, Rong Wang, and Feiping Nie. Multiview clustering: A scalable and parameter-free bipartite graph fusion method. *IEEE Transactions on Pattern Analysis and Machine Intelligence*, 44(1):330–344, 2020.
- [25] Kun-Yu Lin, Ling Huang, Chang-Dong Wang, and Hong-Yang Chao. Multi-view proximity learning for clustering. In *International Conference on Database Systems for Advanced Applications*, pages 407–423. Springer, 2018.
- [26] Guangcan Liu, Zhouchen Lin, Shuicheng Yan, Ju Sun, Yong Yu, and Yi Ma. Robust recovery of subspace structures by low-rank representation. *IEEE Transactions on Pattern Analysis and Machine Intelligence*, 35(1):171–184, 2012.
- [27] Jiani Liu, Ce Zhu, and Yipeng Liu. Smooth compact tensor ring regression. *IEEE Transactions on Knowledge and Data Engineering*, 2020.
- [28] Jiyuan Liu, Xinwang Liu, Yuexiang Yang, Xifeng Guo, Marius Kloft, and Liangzhong He. Multiview subspace clustering via co-training robust data representation. *IEEE Transactions on Neural Networks and Learning Systems*, 2021.
- [29] Suyuan Liu, Siwei Wang, Pei Zhang, Kai Xu, Xinwang Liu, Changwang Zhang, and Feng Gao. Efficient one-pass multi-view subspace clustering with consensus anchors. In *Proceedings of the AAAI Conference on Artificial Intelligence*, volume 36, pages 7576–7584, 2022.
- [30] Yipeng Liu, Jiani Liu, Zhen Long, and Zhu Ce. *Tensor Computation for Data Analysis*. Springer International Publishing, 2021.
- [31] Yu Liu, Quanming Yao, and Yong Li. Generalizing tensor decomposition for n-ary relational knowledge bases. In *Proceedings of The Web Conference 2020*, pages 1104–1114, 2020.
- [32] Zhen Long, Yipeng Liu, Longxi Chen, and Ce Zhu. Low rank tensor completion for multiway visual data. *Signal processing*, 155:301–316, 2019.

- [33] Zhen Long, Ce Zhu, Jiani Liu, and Yipeng Liu. Bayesian low rank tensor ring for image recovery. *IEEE Transactions on Image Processing*, 30:3568–3580, 2021.
- [34] Andrew Y Ng, Michael I Jordan, and Yair Weiss. On spectral clustering: Analysis and an algorithm. In *Advances in Neural Information Processing Systems*, pages 849–856, 2002.
- [35] Feiping Nie, Guohao Cai, and Xuelong Li. Multi-view clustering and semi-supervised classification with adaptive neighbours. In *Thirty-first AAAI Conference on Artificial Intelligence*, 2017.
- [36] Feiping Nie, Jing Li, and Xuelong Li. Parameter-free auto-weighted multiple graph learning: a framework for multiview clustering and semi-supervised classification. In *International Joint Conference on Artificial Intelligence*, pages 1881–1887, 2016.
- [37] Feiping Nie, Jing Li, and Xuelong Li. Self-weighted multiview clustering with multiple graphs. In *International Joint Conference on Artificial Intelligence*, pages 2564–2570, 2017.
- [38] Shi-Ju Ran, Emanuele Tirrito, Cheng Peng, Xi Chen, Luca Tagliacozzo, Gang Su, and Maciej Lewenstein. *Tensor Network Contractions: Methods and Applications to Quantum Many-Body Systems*. Springer Nature, 2020.
- [39] Hinrich Schütze, Christopher D Manning, and Prabhakar Raghavan. *Introduction to information retrieval*, volume 39. Cambridge University Press Cambridge, 2008.
- [40] Yao Sui, Guanghui Wang, and Li Zhang. Sparse subspace clustering via low-rank structure propagation. *Pattern Recognition*, 95:261–271, 2019.
- [41] Ledyard R Tucker. Some mathematical notes on three-mode factor analysis. *Psychometrika*, 31(3):279–311, 1966.
- [42] Ledyard R Tucker et al. The extension of factor analysis to three-dimensional matrices. *Contributions to mathematical psychology*, 110119, 1964.
- [43] Hao Wang, Yan Yang, and Bing Liu. Gmc: Graph-based multi-view clustering. *IEEE Transactions on Knowledge and Data Engineering*, 32(6):1116–1129, 2019.
- [44] Xiaobo Wang, Xiaojie Guo, Zhen Lei, Changqing Zhang, and Stan Z Li. Exclusivity-consistency regularized multi-view subspace clustering. In *Proceedings of the IEEE Conference on Computer Vision and Pattern Recognition*, pages 923–931, 2017.
- [45] Jianlong Wu, Zhouchen Lin, and Hongbin Zha. Essential tensor learning for multi-view spectral clustering. *IEEE Transactions on Image Processing*, 28(12):5910–5922, 2019.

- [46] Jianlong Wu, Xingyu Xie, Liqiang Nie, Zhouchen Lin, and Hongbin Zha. Unified graph and low-rank tensor learning for multi-view clustering. In *Proceedings of the AAAI conference on artificial intelligence*, volume 34, pages 6388–6395, 2020.
- [47] Wei Xia, Quanxue Gao, Qianqian Wang, Xinbo Gao, Chris Ding, and Dacheng Tao. Tensorized bipartite graph learning for multi-view clustering. *IEEE Transactions on Pattern Analysis and Machine Intelligence*, 2022.
- [48] Yuan Xie, Dacheng Tao, Wensheng Zhang, Yan Liu, Lei Zhang, and Yanyun Qu. On unifying multi-view self-representations for clustering by tensor multi-rank minimization. *International Journal of Computer Vision*, 126(11):1157–1179, 2018.
- [49] Yuan Xie, Wensheng Zhang, Yanyun Qu, Longquan Dai, and Dacheng Tao. Hyper-laplacian regularized multilinear multiview self-representations for clustering and semisupervised learning. *IEEE transactions on cybernetics*, 50(2):572–586, 2020.
- [50] Yan Yang and Hao Wang. Multi-view clustering: A survey. *Big Data Mining and Analytics*, 1(2):83–107, 2018.
- [51] Yuyuan Yu, Guoxu Zhou, Ning Zheng, Shengli Xie, and Qibin Zhao. Graph regularized nonnegative tensor ring decomposition for multiway representation learning. *arXiv preprint arXiv:2010.05657*, 2020.
- [52] Longhao Yuan, Jianting Cao, Xuyang Zhao, Qiang Wu, and Qibin Zhao. Higher-dimension tensor completion via low-rank tensor ring decomposition. In *2018 Asia-Pacific Signal and Information Processing Association Annual Summit and Conference (APSIPA ASC)*, pages 1071–1076. IEEE, 2018.
- [53] Changqing Zhang, Huazhu Fu, Si Liu, Guangcan Liu, and Xiaochun Cao. Low-rank tensor constrained multiview subspace clustering. In *Proceedings of the IEEE International Conference on Computer Vision*, pages 1582–1590, 2015.
- [54] Changqing Zhang, Huazhu Fu, Jing Wang, Wen Li, Xiaochun Cao, and Qinghua Hu. Tensorized multi-view subspace representation learning. *International Journal of Computer Vision*, 128(8):2344–2361, 2020.
- [55] Changqing Zhang, Qinghua Hu, Huazhu Fu, Pengfei Zhu, and Xiaochun Cao. Latent multi-view subspace clustering. In *Proceedings of the IEEE Conference on Computer Vision and Pattern Recognition*, pages 4279–4287, 2017.
- [56] Guang-Yu Zhang, Yu-Ren Zhou, Chang-Dong Wang, Dong Huang, and Xiao-Yu He. Joint representation learning for multi-view subspace clustering. *Expert Systems with Applications*, 166:113913, 2021.

- [57] Qibin Zhao, Guoxu Zhou, Shengli Xie, Liqing Zhang, and Andrzej Cichocki. Tensor ring decomposition. *arXiv preprint arXiv:1606.05535*, 2016.
- [58] Qinghai Zheng and Jihua Zhu. Multi-view subspace clustering with view correlations via low-rank tensor learning. *Computers and Electrical Engineering*, 100:107939, 2022.
- [59] Qinghai Zheng, Jihua Zhu, Zhiqiang Tian, Zhongyu Li, Shanmin Pang, and Xiuyi Jia. Constrained bilinear factorization multi-view subspace clustering. *Knowledge-Based Systems*, 194:105–514, 2020.
- [60] Shi Zhong and Joydeep Ghosh. A unified framework for model-based clustering. *The Journal of Machine Learning Research*, 4:1001–1037, 2003.
- [61] Wenzhang Zhuge, Feiping Nie, Chenping Hou, and Dongyun Yi. Unsupervised single and multiple views feature extraction with structured graph. *IEEE Transactions on Knowledge and Data Engineering*, 29(10):2347–2359, 2017.